

Numerical Study of Super-Cooled Droplet Impingement on Aeroengine

Yan TAN*, Wuguo WEI**

*Civil Aviation Flight University of China, Guanghan 618307, China, E-mail: tanyan_cafuc@sina.com

**Civil Aviation Flight University of China, Guanghan 618307, China, E-mail: weiwuguo@163.com

crossref <http://dx.doi.org/10.5755/j01.mech.26.1.23107>

Nomenclature

α is volume factor ($\alpha=V_d/V$); V is control volume, m^3 ; \mathbf{u} is velocity vector, m/s ; \mathbf{G} is droplet gravity vector, m/s^2 ; K is momentum exchange coefficient; μ is dynamic viscosity of air, $kg/(m \cdot s)$; ρ is density, kg/m^3 ; d is diameter of droplet, m ; Re is relative Reynolds number; C_D is drag coefficient; K_C is Cossali number ($K_C=WeOh^{-2/5}$); n is droplet number; Oh is Ohnesorge number; We is Weber number.

Subscripts: d is droplet; a is air; s is after splashing.

1. Introduction

When aircraft is flying in clouds, fogs, rain or snow, ice accretion will occur on the surface of the wing, fuselage and engine due to the super-cooled droplets impingement. This phenomenon causes air accidents and personnel losses almost every year. In 1994, the air accident of American Eagle Flight 4184 was a milestone event. People began to pay attention to the effect of SLD (Super-cooled Large Droplet) impingement on aircraft icing. SLD usually has a diameter greater than $40 \mu m$. Due to aerodynamic effects, deformation, breakage and bounce will occur when the SLD impact on aircraft surface. These phenomena will change the droplet trajectory and collection efficiency, which has a great influence on icing growth.

In view of the above reasons, scholars have carried out SLD related researches in the past 20 years. The representative works are as follows. Gent [1] and Potapczuk [2] investigated the relationship between droplet size and mass loss caused by splashing based on experimental method. Tan [3] and Feo [4] used CCD (Charge Couple Device) technology to record the droplet splashing characteristics. Some important results were also obtained by numerical method. The method of impingement property calculation could be divided into Lagrange method [5-6] and Euler method [7-9]. The Lagrange method could capture the deformation of single droplet. But it is difficult to determine the particle release location for complicated shape, and the calculation amount is large. However the Euler method doesn't have these problems. Most of the above works took the simpler shapes (such as wing) as research objects. While the aeroengine has complicated structure and flow field, and the study of aeroengine icing has always been a difficult point. The open literature is relatively less. Farag [10] developed BETAPROP software for calculating the impingement property on propeller surfaces. Bidwell [11] used LEWICE 3D to calculate the droplet collection efficiency of Boeing 737-700's engine inlet. Isobe [12] obtained the droplet collection efficiency on fan blade based on Lagrange method. It could be found that the exiting works mainly focused on single part such as engine inlet lip and fan blade. However, there were few systematic studies on the ice-

prone parts of the engine.

In this paper, a certain type of aeroengine was taken as the research object. The impingement of super-cooled droplets including SLD on nose cone, fan blade, guide vanes in bypass and core duct were studied based on Euler method. The data of LWC (Liquid Water Content) and droplet collection efficiency of each part were obtained. The effect of droplet size on impingement property of engine icing-prone parts was analyzed.

2. Model development

Firstly, the three dimensional engine flow field result was obtained by Spalart-Allmaras turbulence model [13]. Then the impingement property was analyzed based on Euler multiphase flow model. The continuity and momentum equations are as follows:

$$\nabla \cdot (\rho_d \alpha \mathbf{u}_d) = 0, \quad (1)$$

$$\nabla \cdot (\rho_d \alpha \mathbf{u}_d \mathbf{u}_d) = \rho_d \alpha K (\mathbf{u}_a - \mathbf{u}_d) + \rho_d \alpha \mathbf{G}_d, \quad (2)$$

where: K is momentum exchange coefficient between air and droplet (Eq. (3)). The Eq. (1) and Eq. (2) are solved by Streamline-Upwind Petrov- Galerkin method [14]:

$$K = \frac{18\mu_a}{\rho_d d^2} \cdot \frac{C_D Re}{24}, \quad (3)$$

$$Re = \frac{\rho_a d \|\mathbf{u}_a - \mathbf{u}_d\|}{\mu_a}, \quad (4)$$

$$C_D = \begin{cases} 24(1 - 0.15 Re^{0.687}) / Re & Re \leq 1300 \\ 0.44 & Re > 1300 \end{cases}. \quad (5)$$

The difference between SLD and ordinary droplets is that the splashing and bouncing will occur after impingement. Here, the splashing phenomenon is judged by the criterion proposed by Mundo [15]. When, $K_M = K_C^{0.625} > 57.5$, splashing occurs and the parameters of new droplet are shown in Eq. (6-8). After splashing the normal and tangential velocities of new droplet are equal to those of droplet before impingement:

$$d_s / d = 8.72e^{-0.028K_M}, \quad (6)$$

$$n_s = 1.676 * 10^{-5} K_M^{2.539}, \quad (7)$$

$$\frac{LWC_s}{LWC} = n_s \left(\frac{d_s}{d} \right)^3. \quad (8)$$

When, $2 < We < 20$, the bouncing phenomenon occur, and $d_s = d$, $LWC_s = LWC$.

3. Case study

In this paper, a large bypass ratio engine was taken

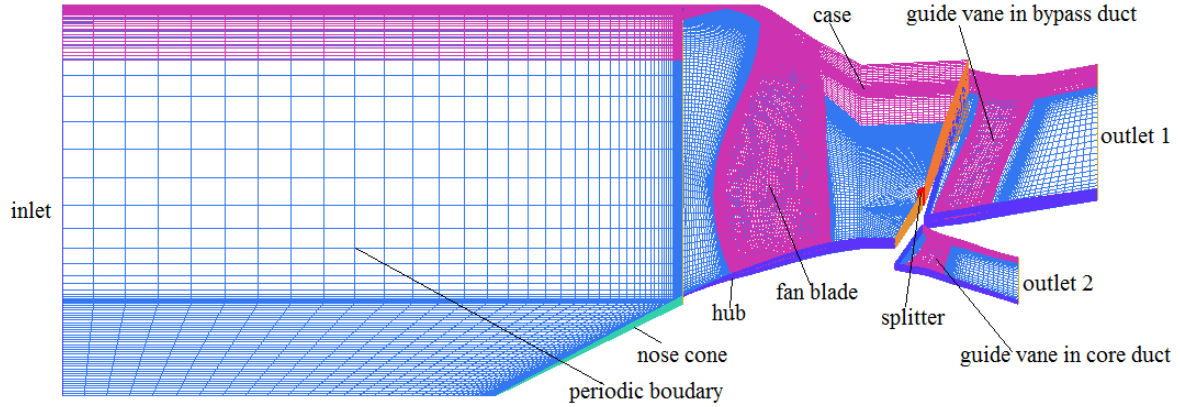


Fig. 1 Aeroengine grid models

Usually, the ice accretion occurs in the take-off or landing phase. Therefore, the impingement property under a typical working condition (3000 m altitude) was calculated. The computational conditions are summarized in Table 1. The 1/8 nose cone model was established in this paper; therefore, the mass flow was 1/8 of the original. Meanwhile, the droplet distribution (Fig. 2) was selected according to the recommendation from FAR Appendix O.

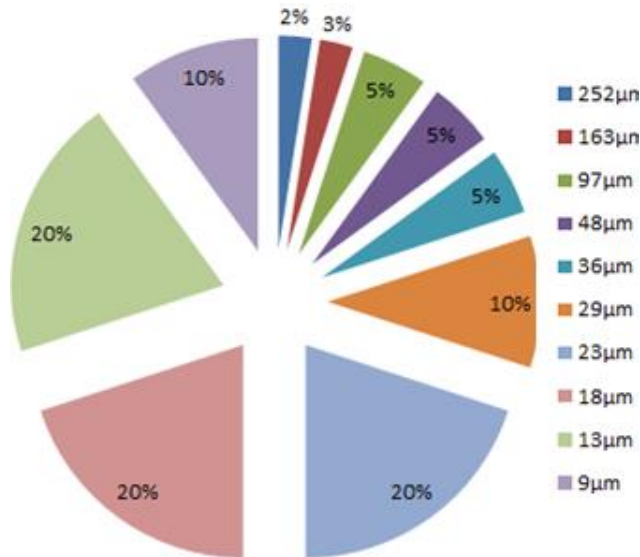


Fig. 2 Droplet distribution

Table 1

Working conditions of calculation

Condition	Value
Inlet mass flow, kg/s	135
Inlet total temperature, K	266
Outlet static pressure 1, Pa	79500
Outlet static pressure 2, Pa	79800
LWC, g/m ³	0.3
Fan speed, rpm	2580

as the research object. The grid models (1.2 million structural grids) were established, including the nose cone, fan, guide vane in bypass duct and in core duct. Because the number of fan blades and guide vanes was different, the above components were modelled separately in this paper. The data exchange between them was realized by mixed boundary. The whole mode after assembly is shown in Fig. 1.

4. Analysis of numerical results

For the convenience of analysis, the results of four types of droplets with different diameters (252, 48, 23 and 9 μm, the first two droplets were typical SLD) were discussed.

Fig. 3 shows the LWC contour at different radial positions in the fan section. Here, the region colored by blue is called the shadow zone, where no droplets exist. It could be found that the smaller the droplet is, the closer the shadow zone is to the cone, which is caused by droplet inertia. The SLD is difficult to change the original trajectory due to its high inertia, impinges on the windward side (Fig. 4, a). Therefore, there is no obvious LWC gradient (Fig. 4, b). However, the small droplet is easy to change the trajectory (Fig. 4, c). A large number of droplets gather in the boundary layer and move backward, which causes high LWC value in the boundary layer of cone. In addition, a narrow shadow zone is formed at the rear of the cone due to the shrinkage of the hub shape (Fig. 4, d). It also could be found that the fan blade's AOA (Angle of Attack) increases gradually from the root to the tip, the shadow zone narrows gradually. Similarly, the smaller the droplet is, the narrower the shadow zone is, due to the droplet inertia. And there is a higher LWC concentration region will appear at the tip trailing edge due to the centrifugal force and case's limitation.

Droplet collection efficiency reflects the probability of droplet impinges on the surface. It is an important parameter for ice accretion calculation, and also one of the important indicators of the distribution and severity of surface icing. Fig. 5 shows the contour of droplet collection efficiency with different diameters. It could be found that the larger the droplet, the greater the impingement probability on the cone. There is almost no droplet impinges on the fan blade's convex side except for sweep forward part where a few droplets impinge on. The droplets mainly impinge on

the concave side. The larger the droplet, the larger the impingement area is. However, the droplets impinge on the convex side of guide vanes in bypass duct and core duct. The impingement area reduces with the droplet size, extends from the upper guide vane to the lower one, and becomes

narrower gradually. The above phenomena are mainly caused by inertia. The SLD has difficulty to change the trajectory, therefore the structure is more likely to be impinged by larger droplet. Meanwhile the SLD affected by centrifugal force leaves the engine from bypass duct.

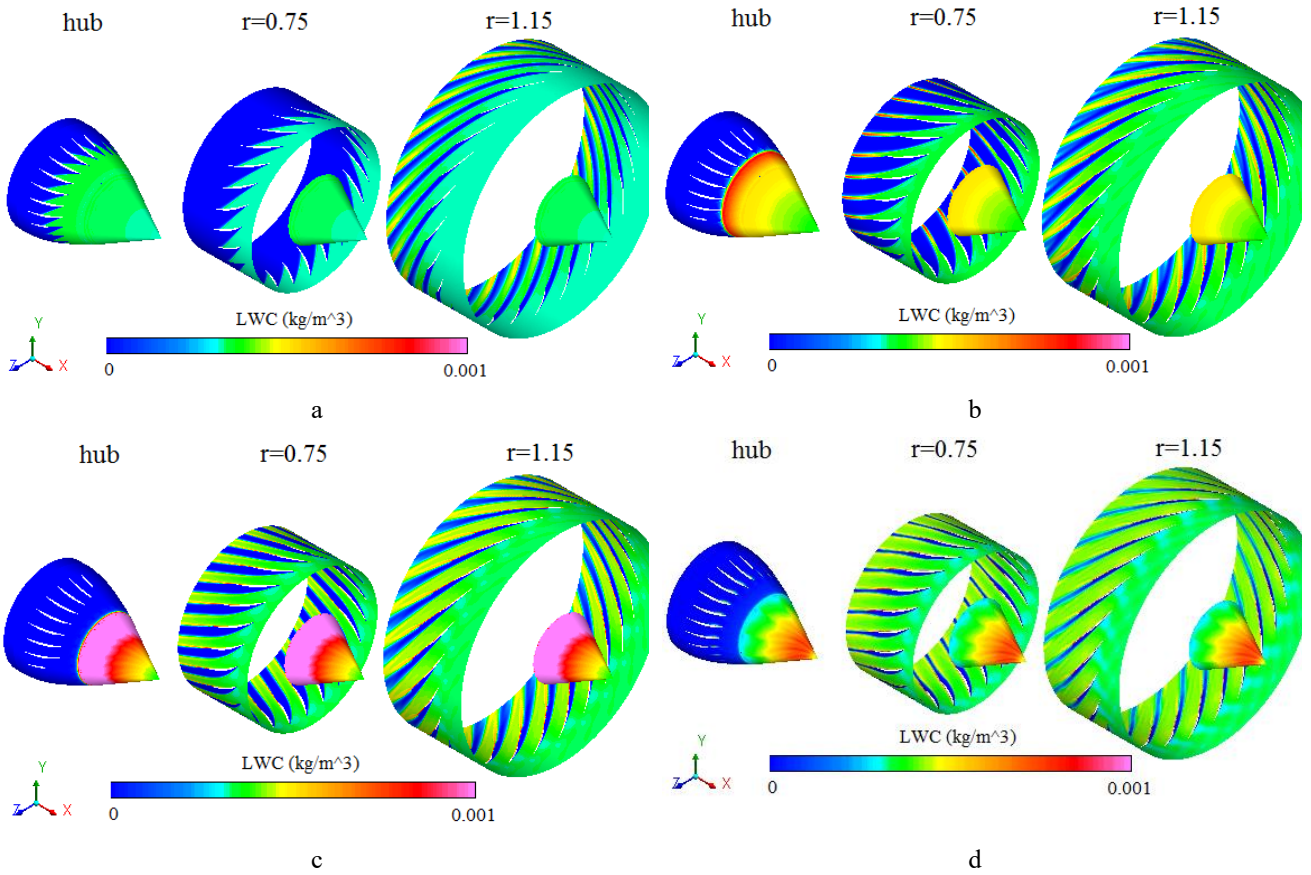


Fig. 3 LWC contour (a - 252 μm ; b - 48 μm ; c - 23 μm ; d - 9 μm)

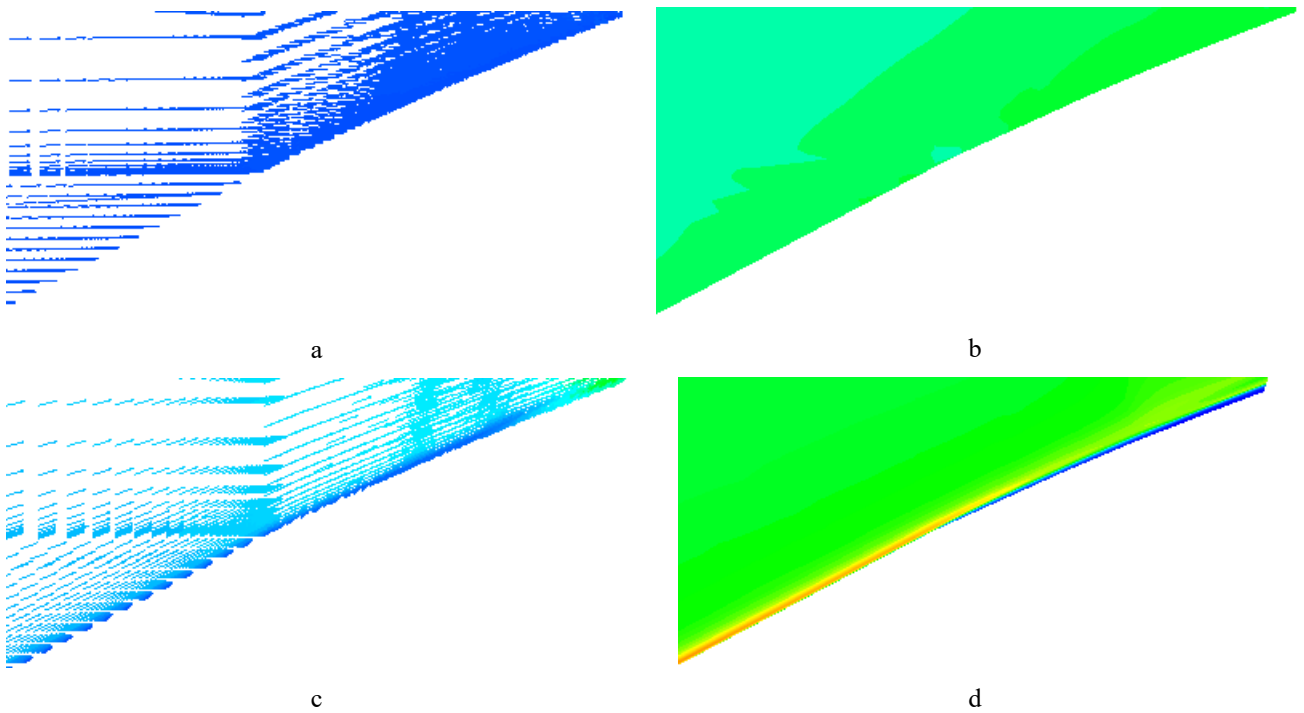


Fig. 4 Velocity vector and LWC contour of cone's surface flow field (a - velocity vector of 252 μm ; b - LWC contour of 252 μm ; c - velocity vector of 9 μm ; d - LWC contour of 9 μm)

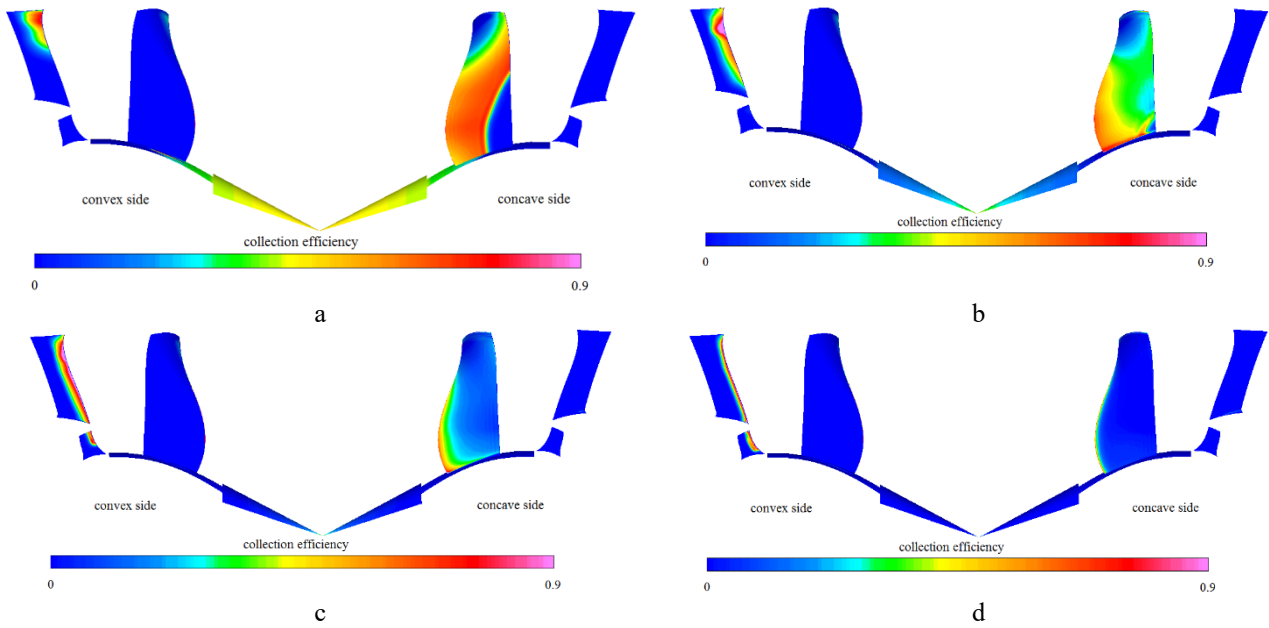


Fig. 5 Droplet collection efficiency contour (a - 252 μm ; b - 48 μm ; c - 23 μm ; d - 9 μm)

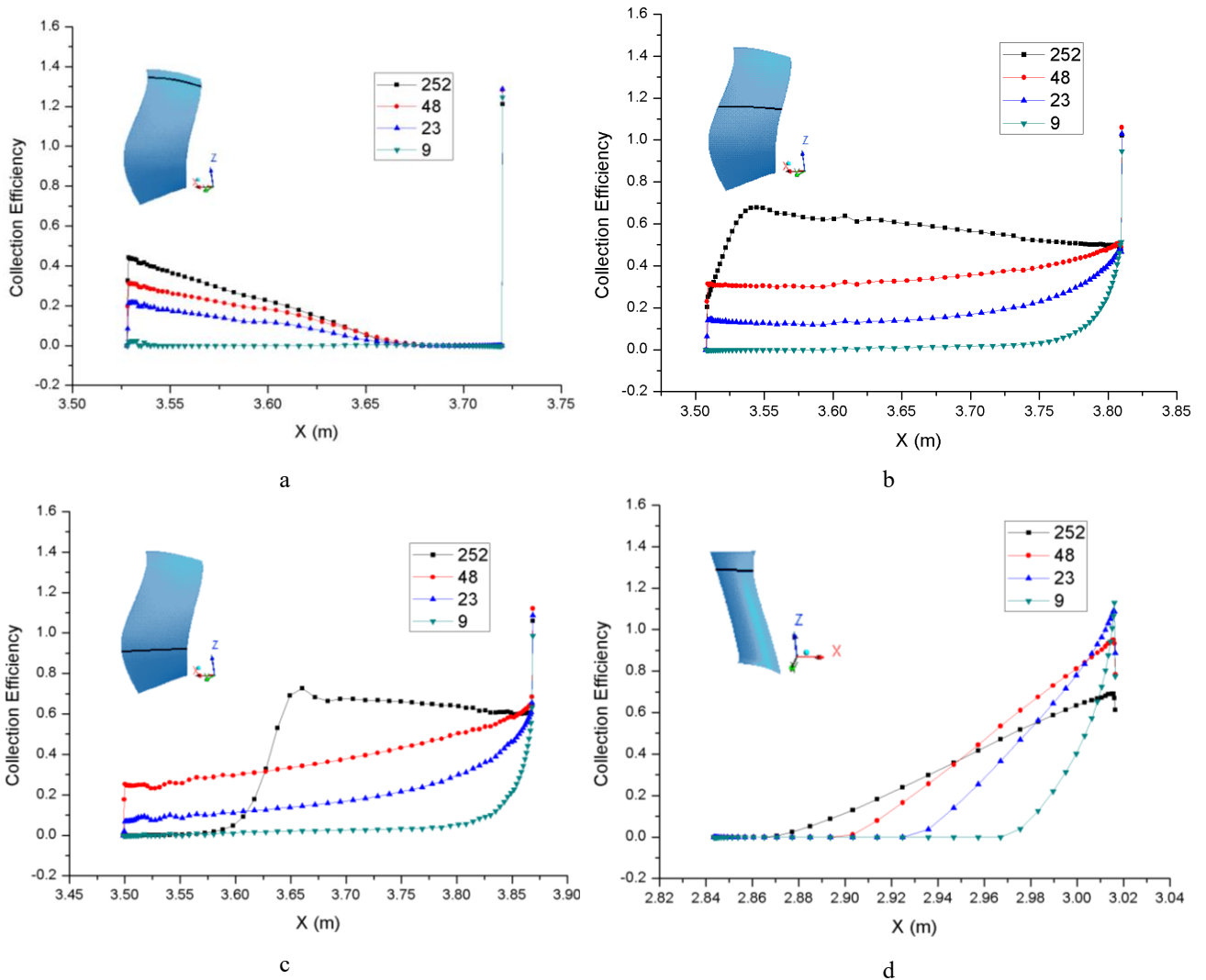


Fig. 6 Comparison of droplet collection efficiency (a - upper part of fan blade (concave side); b - middle part of fan blade (concave side); c - lower part of fan blade (concave side); d - upper part of guide vane in bypass duct (convex side); e - middle part of guide vane in bypass duct (convex side); f - lower part of guide vane in bypass duct (convex side); g - upper part of guide vane in core duct (convex side); h - lower part of guide vane in core duct (convex side))

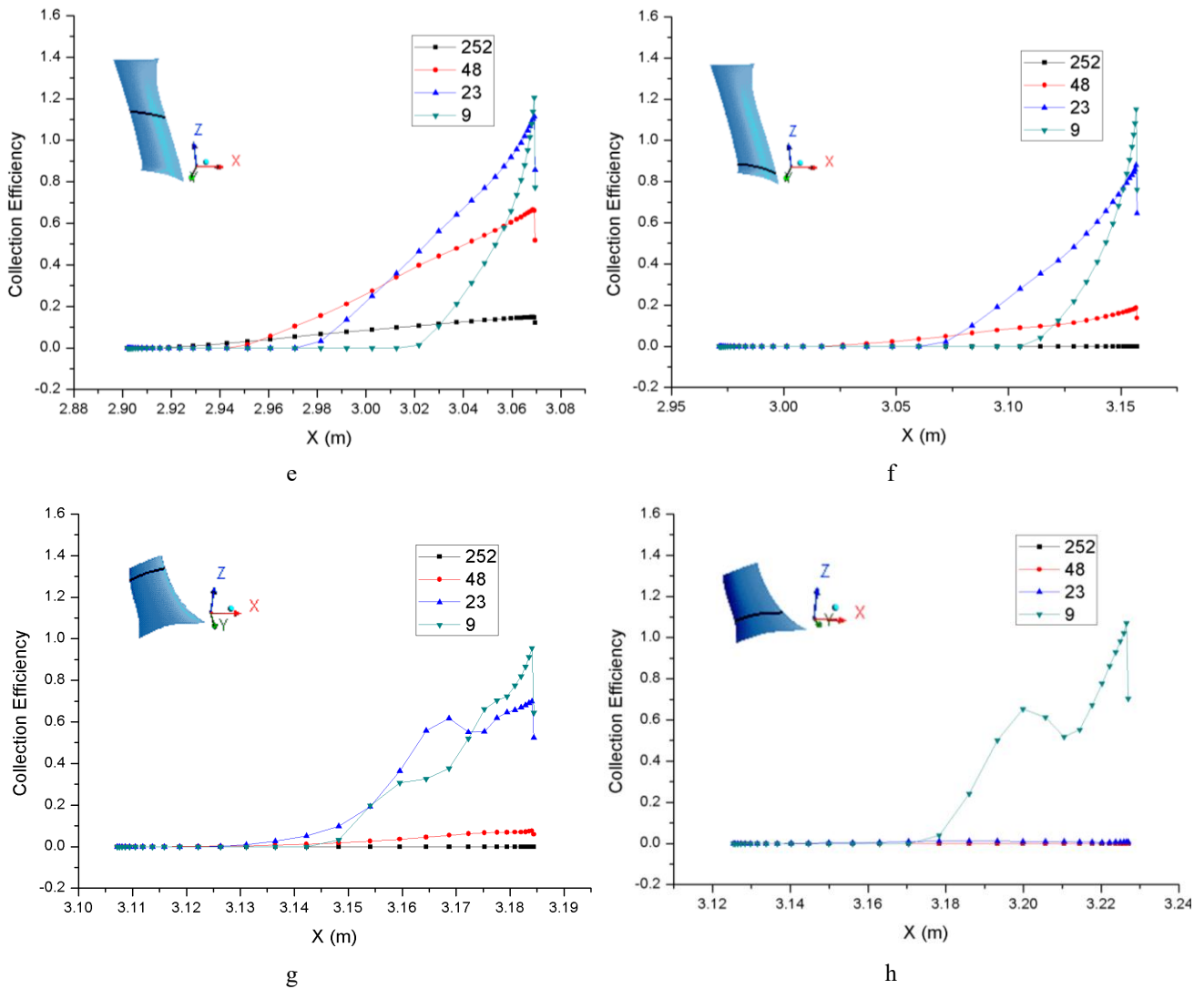


Fig. 6 Continuation

Fig. 6 shows the comparison of droplet collection efficiency on different blades and locations. The impingement probability of SLD is greater than others due to the high inertia. The smaller the droplet is, the closer the impingement site to the blade root and the closer to the leading edge. It is noteworthy that the LWC value near the trailing edge of blade tip increases gradually (Fig. 6, a). The LWC concentration appeared at the tip trailing edge due to centrifugal force and case's limitation, which greatly increases the probability of droplet impacting the rear tip of blade (Fig. 3). In addition, most of the droplets with 252 μm subject to centrifugal force, which will result in the collection efficiency's cliff-like drop (Fig. 6, b-c).

The location of maximum collection efficiency moves backward due to the stagnation point shifts to the convex side. The collection efficiency of bypass and core duct is mainly contributed by small droplets. While the SLD only affects the local part of guide vane in bypass duct, and has little effect on the guide vane in core duct (Fig. 6, d-h).

5. Conclusions

In this paper, the Euler method was used to calculate the droplet impingement property of a large bypass ratio aeroengine. The LWC and droplet collection efficiency in different parts were obtained by this method. The large

droplets are mainly impinging on the fan blade's concave side, and only affected the local part of guide vane in bypass duct due to centrifugal force. While the small droplets impinging the guide vanes in bypass duct and core duct. The results could provide some references for subsequent engine icing calculation and anti-icing system design.

Acknowledgements

This work supported by the Scientific Research Foundation of CAFUC (Grant No. J2019-60).

References

1. **Gent, R.; Ford, J. M.; Moser, R. J.; Miller, M. D.** 2003. Results from Super-cooled large droplet mass loss tests in the ACT Luton icing wind tunnel, AIAA 2003-389.
2. **Potapczuk, M. G.** 2003. Ice mass measurements: implications for the ice accretion process, AIAA 2003-387.
3. **Tan, S. C.; Papadakis, M.; Miller, M. D.** 2007. Experimental study of large droplet splashing and breakup, AIAA 2007-904.
4. **Fo, A.; Vargas, M.; Sor, A.** 2011. Rotating rig development for droplet deformation/breakup and impact induced by aerodynamic surfaces, SAE 2011-38-0087.

5. **Tan, S. C.** 2004. A tentative mass loss model for simulating water droplet splash, AIAA 2004-0410.
6. **Wright, W. B.; Potapczuk, M. G.** 2004 Semi-empirical modelling of SLD physics, AIAA 2004-412.
7. **Iuliano, E.; Mingione, G.; Petrosino, F.; Hervy, F.** 2011. Eulerian modeling of large droplet physics toward realistic aircraft icing simulation, *Journal of Aircraft* 48(5): 1621-1632.
<http://dx.doi.org/10.2514/1.C031326>.
8. **Honsek, R.; Habashi, W. G.; Aube, M. S.** 2008. Eulerian modeling of in-flight icing due to supercooled large droplets, *Journal of Aircraft* 45(4): 1290-1296.
<http://dx.doi.org/10.2514/1.34541>.
9. **Bilodeau, D. R.; Habashi, W. G.; Fossati, M.; Baruzzi, G. S.** 2015. Eulerian modeling of supercooled large droplet splashing and bouncing, *Journal of Aircraft* 52(5): 1611-1624.
10. **Farag, K.; Bragg, M. B.** 1998. Three dimensional droplet trajectory code for propellers of arbitrary geometry, AIAA 1998-0197.
11. **Bidwell, C. S.** 1996. Collection efficiency and ice accretion calculations for a Boeing 737-300 inlet, NASA TM-107347.
12. **Isobe, K.; Suzuki, M.; Yamamoto, M.** 2014. Numerical investigation on super-cooled large droplet icing of fan rotor blade in jet engine, *Journal of Thermal Science* 23(5): 432-437.
13. **Spalart, P. R.; Allmaras, S. R.** 1992. A one-equation turbulence model for aerodynamic Flows, AIAA 1992-0439.
14. **Hughes, T. J. R.; Brooks, A.** 1982. A Theoretical Framework for Petrov-Galerkin Methods with Discontinuous Weighting Functions: Application to the Streamline-Upwind Procedure, Wiley press. 647 p.
<http://dx.doi.org/10.1007/s11630-014-0726-2>.
15. **Mundo, C.; Tropea, C.; Sommerfeld, M.** 1997. Numerical and experimental investigation of spray characteristics in the vicinity of a rigid wall, *Experimental Thermal and Fluid Science* 15(3): 228-237.
[http://dx.doi.org/10.1016/S0894-1777\(97\)00015-0](http://dx.doi.org/10.1016/S0894-1777(97)00015-0).

Y. Tan, W. Wei

NUMERICAL STUDY OF SUPER-COOLED DROPLET IMPINGEMENT ON AEROENGINE

S u m m a r y

In this work, a large bypass ratio engine is taken as the research object. The impingement property of droplets with various diameters including SLD (Super-cooled Large Droplet) is obtained by Euler method based on Mundo model. The grid models of nose cone, fan, guild vanes in bypass duct and core duct are established in segments firstly. The mixed boundary is used to realize the data exchange between different flow fields. Then the Spalart-Allmaras turbulence model was applied to calculate the three dimensional engine flow field. Based on the flow field result, the droplet trajectory is calculated by Euler multi-phase flow method. The LWC (Liquid Water Content), droplet collection efficiency and the effect of droplet diameter on impingement law are obtained. It could be found that the large droplets mainly impinge on the fan blade's concave side and local part of guide vane in bypass duct. With the droplet's diameter decreasing, the impingement range extends to the leading edge of entire fan, guild vanes in bypass duct and core duct. The method used in this paper and results could provide some references for subsequent engine icing calculation and anti-icing system design.

Keywords: aeroengine, super-cooled droplet, numerical simulation, impingement property.

Received April 07, 2019

Accepted February 03, 2020